

INFLUENCE OF THERMAL AGEING ON FATIGUE CRACK GROWTH BEHAVIOUR IN CAST DUPLEX STAINLESS STEELS

V. Calonne, A.F. Gourgues and A. Pineau

Centre des Matériaux P.M. Fourt, Ecole des Mines de Paris, UMR CNRS 7633
BP 87, 91003 Evry Cedex, France
e-mail : virginie.calonne@mat.ensmp.fr

ABSTRACT

Duplex stainless steels ($\approx 30\%$ ferrite α , $\approx 70\%$ austenite γ) are largely used as cast components in nuclear power plants. These materials which may have equiaxed and basaltic solidification structures can be embrittled at the service temperature of about 320°C . The effects of this embrittlement and of solidification structure on Fatigue Crack Growth Rate (FCGR) behaviour were investigated in two cast materials which had been previously aged under different conditions.

It is shown that the FCGR as a function of ΔK is increased by ageing when the material is brittle enough. On the contrary crack closure is decreased by ageing. Therefore, FCGR as a function of ΔK_{eff} are similar. Crack closure effect is induced by roughness and plasticity. The differences in crack closure levels can partly be related to the differences in cyclic hardening behaviour.

In equiaxed grains or in a plane parallel to basalts, crack propagates at the same speed, expressed as a function of ΔK , but in a plane perpendicular to basalts, it propagates more quickly. The FCGR differences can be explained by the more or less tortuous aspect of the crack.

No preferential crack propagation path between the two phases is evidenced but macroscopic crack path corresponds to the $\{100\}$ ferrite cleavage planes when aged and to the $\{123\}$ ferrite slip planes when unaged.

INTRODUCTION

Duplex stainless steels containing up to 30% of ferrite (α) in an austenitic matrix (γ) are used for the fabrication of pipes in nuclear power plants. These materials combine the qualities of each phase : the ferrite resistance to corrosion and to hot cracking and the austenite toughness [1]. It has been established that microstructural transformations occur in ferrite after long time exposures ($> 10\,000$ h) at service temperature of about 320°C . The main transformations are the demixtion of α in α and α' , a chromium-rich phase, and the precipitation of a G phase ($\text{Ni}_{16}\text{Ti}_6\text{Si}_7$) [2]. As a consequence, ferrite becomes hard and brittle which induces a significant decrease in toughness and tensile ductility. Moreover, cast components may contain small manufacturing defects from which cracks can be initiated under in-service or incidental conditions. The structural integrity assessment of these components requires therefore that the fatigue crack growth behaviour (FCGB) is taken into account. Several studies have already been performed on this topic but generally, the materials studied contain a high fraction of ferrite (around 50%) and have a different microstructure because hot rolled [3-6]. In the present paper, the influences of ageing and of solidification structure on the FCGB of cast duplex stainless steels containing about 30% ferrite are investigated.

MATERIALS AND EXPERIMENTAL PROCEDURES

Materials

The fatigue crack growth characterisation has been carried out on two different statically cast stainless steel elbows : elbow n°1 having the following chemical composition (wt%) : C=0.033; N=0.057; Cr=21.68; Ni=9.61; Mo=2.64; Si=0.94; Mn=0.82; P=0.023; S=0.0005 and elbow EK : C=0.034; N=0.054; Cr=21.20; Ni=9.70; Mo=2.51; Si=1.07; Mn=0.88; P=0.018; S=0.004. These components contain almost the same ferrite volume fraction : 32% for elbow n°1 and 28% for elbow EK.

Because of static casting manufacturing process, the solidification structure is basaltic near the surface and equiaxed in the bulk (Figure 1). The typical microstructure is shown in Figure 2.a. Electron Back Scatter Diffraction (EBSD) was used to study the material structure. This technique enables to determine local crystallographic orientations. It has been shown that ferrite grain is convex and of size of around 2 mm for elbow n°1 and of around 4 mm for elbow EK. In equiaxed area, grain orientation is random but in basaltic area, basalts are oriented along $\langle 100 \rangle_{\alpha}$ directions. The austenitic grain structure is more complex as shown in Figure 2.b. These grains are not convex and there is no unique correspondance between the morphological orientation of the lathes and their crystallographic orientation. The orientation relationships between α and γ are close to those given by Kurdjumov-Sachs [7], i.e. one $\{111\}_{\gamma} //$ one $\{110\}_{\alpha}$ and in that plane, one $\langle 110 \rangle_{\gamma} //$ one $\langle 111 \rangle_{\alpha}$ (Figure 2.c).

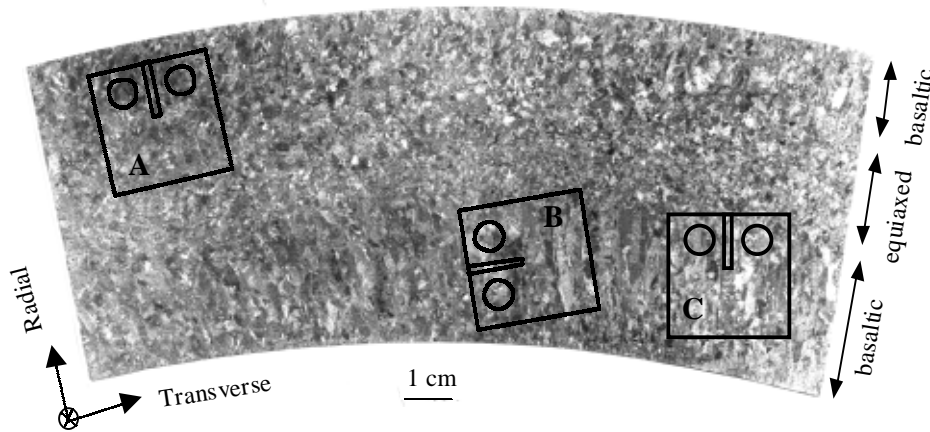


Figure 1 : Solidification structure of a statically cast elbow and orientation of the crack plane for the different kinds of specimens : A : equiaxed grains, B : perpendicular to basaltic grains, C : parallel to basaltic grains.

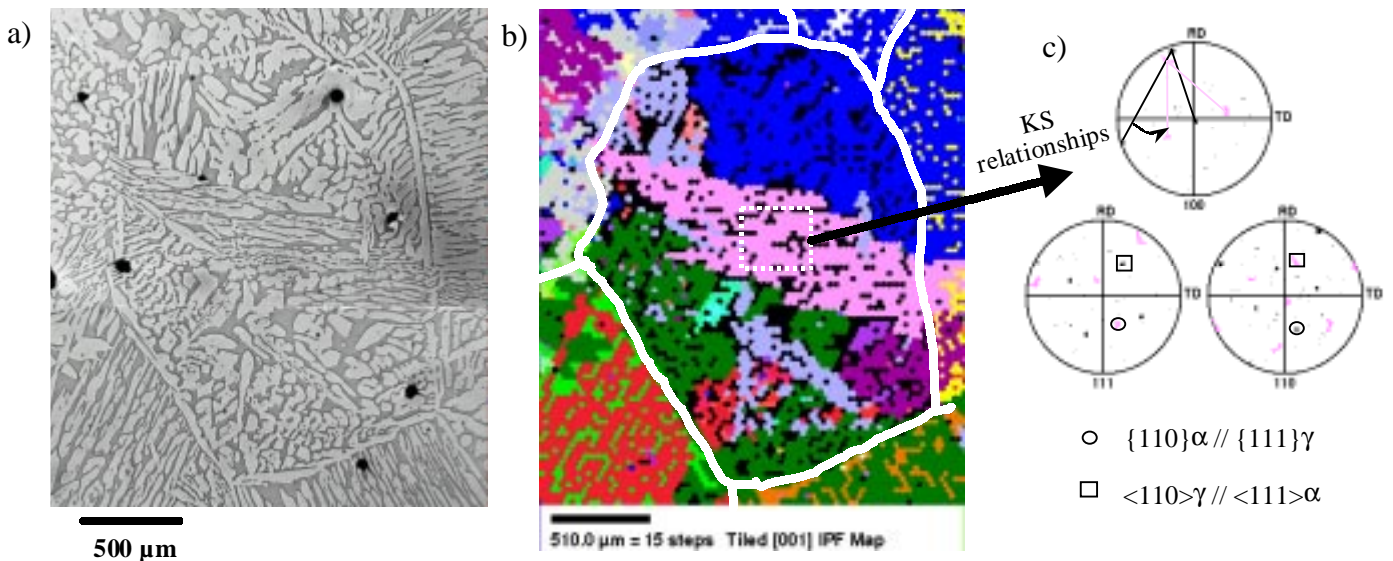


Figure 2 : Microstructure of equiaxed grains of static cast duplex stainless steel: a) optical micrographs (ferrite = grey, austenite = light); b) EBSD map (one colour corresponds to one crystallographic orientation, white lines = limits of α grains); c) corresponding pole figures.

Elbows n°1 and EK were aged at 400°C for 2 400 hours and 10 000 hours, respectively. Both materials were also tested after a solution-annealing heat treatment at 1 100°C for 3 hours followed by water quenching. These materials are called unaged. Mechanical properties are given in Table 1.

		Yield Stress (0.2% strain) MPa	Ultimate Tensile Stress MPa	Strain to Failure (%)	Reduction of area (%)	Charpy U Toughness (daJ/cm ²)
elbow n°1	unaged	331	616	42	72	23
	aged	356	762	14	20	2
elbow EK	unaged	340	620	40	52	20
	aged	356	644	5	-	1

Table 1 : Tensile properties and Charpy U toughness at room temperature for aged and unaged elbows n°1 and EK.

It is worth noting that aged elbow n°1 exhibits a Charpy toughness twice as high as that of aged elbow EK. Aged elbow n°1 is then less brittle than aged elbow EK.

Experimental procedures

Fatigue crack propagation tests

CT specimens (W = 40 mm, B = 10 mm) were tested in air at room temperature under sine wave loading with a 0.1 constant load ratio P_{\min}/P_{\max} and a 20 Hz frequency. Crack length was measured by DC potential drop technique.

During tests, crack closure was measured by the compliance method. The crack closure/opening load (P_{op}) is the load above which the crack front is fully opened. So crack propagates only for an applied load varying between P_{op} and P_{\max} and not between P_{\min} and P_{\max} . It is then more accurate to express Fatigue Crack Growth Rates (FCGR) as a function of ΔK_{eff} ($\Delta K_{eff} = K_{\max} - K_{op} = K_{\max} (1 - K_{op}/K_{\max})$) than as a function of ΔK ($\Delta K = K_{\max} - K_{\min}$). K_{\max} , K_{\min} and K_{op} are stress intensity factors at maximum load, minimum load and opening load, respectively.

Fatigue crack growth tests were performed in aged and unaged elbows n°1 and EK. In elbow EK, crack propagation was investigated in the equiaxed structure. In elbow n°1, FCGR was studied not only in the equiaxed structure but also along directions parallel and perpendicular to basaltic grains (Figure 1).

Low cycle fatigue tests

Low cycle fatigue (LCF) tests were carried out in air at room temperature under fully reversed total strain control at a constant total strain rate of 10^{-3} s^{-1} . Strain was measured using a clip-on extensometer. The cyclic stress-strain response of the material was determined by increasing step by step the total strain amplitude from 0.3% to 1.5%.

LCF specimens were cut from equiaxed aged and unaged elbow n°1 and from aged elbow EK.

FATIGUE CRACK GROWTH RATES

Influence of ageing

The effect of ageing on FCGR as a function of ΔK is evidenced in figure 3 for equiaxed microstructures. In the investigated ΔK range, crack growth rates in aged elbow EK are three times larger than in unaged material. On the contrary, for elbow n°1, crack growth rates for aged and unaged materials are close. As aged elbow n°1 is less brittle than aged elbow EK, an influence of ageing on FCGR could be expected at higher ΔK . It can be noticed that the FCGR of unaged elbow n°1 is higher than that of unaged elbow EK.

The ratio K_{op}/K_{\max} is decreasing with ΔK and ageing (figure 4). This largely explains why the FCGR as a function of ΔK_{eff} is independent of ageing (figure 5). As a conclusion, in equiaxed materials, the influence of ageing on the FCGR is mainly correlated to an influence of ageing on crack closure level and not on the intrinsic FCGR.

Influence of solidification induced structure

FCGR are the same when the crack propagates in equiaxed structure (A) or in a plane parallel to basalts (C) (Figure 6). The only difference is that, when the crack propagates in equiaxed structure, an average is made on growth rates in the various ferritic grains of the specimen but when the crack propagates in a plane parallel to basalts, the growth rate depends on the ferritic grain. The scatter is then less important in the first case. When crack propagates in a plane perpendicular to basalts (B), FCGR is six times higher than when it propagates in equiaxed grains. Unfortunately, it has been impossible to measure crack closure for specimen of B type. Crack closure levels in A and C types were found to be similar.

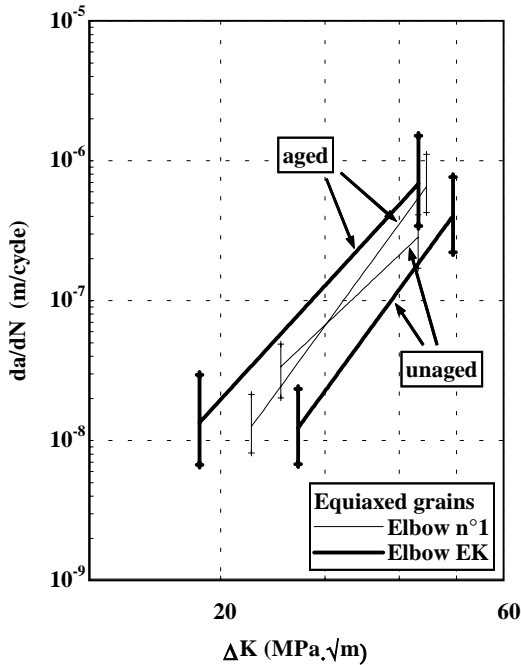


Figure 3 : Crack growth rates as a function of stress intensity factor range ΔK for aged and unaged elbows n°1 and EK with equiaxed grains.

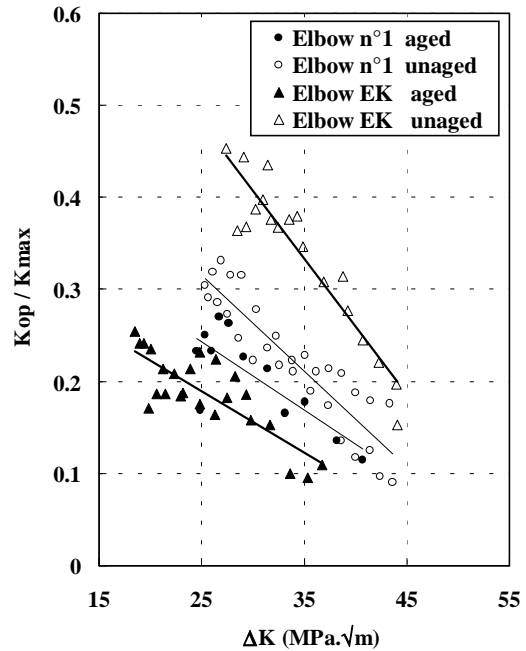


Figure 4 : Variation of the ratio crack opening to maximum stress intensity factors with ΔK for aged and unaged elbows n°1 and EK with equiaxed grains.

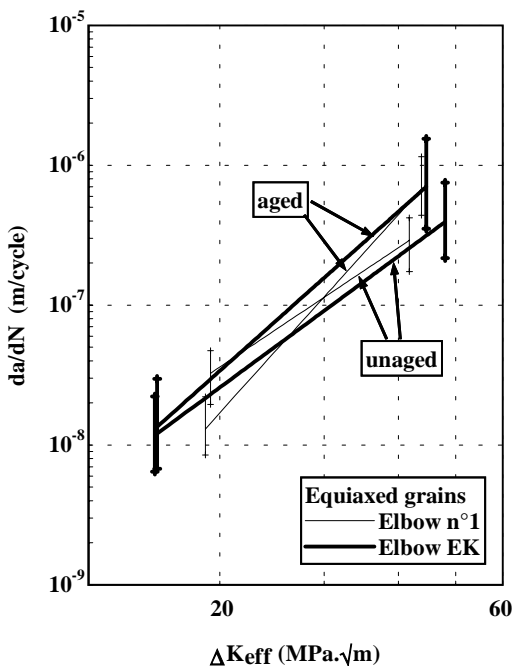


Figure 5 : Crack growth rates as a function of the effective stress intensity factor range ΔK_{eff} for aged and unaged elbows n°1 and EK with equiaxed grains.

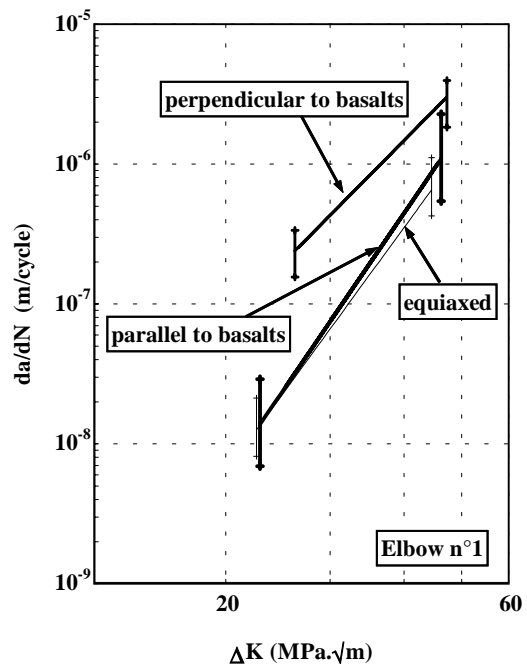


Figure 6 : Crack growth rates as a function of stress intensity factor range ΔK for aged elbow n°1 with different solidification structures.

CRACK CLOSURE

Four main types of crack closure mechanisms are usually considered [8] : i) plasticity induced crack closure (PICC), ii) roughness induced crack closure (RICC), iii) oxide induced crack closure (OICC), iv) transformation induced crack closure (TICC).

As tests have been performed at room temperature on stainless steels, OICC is limited. TICC effect could exist. It is known that, in austenitic stainless steels, the formation of transformation induced martensite as a result of plastic strain can occur at the crack tip [9]. But EBSD observations of the cracks did not show the existence of martensite even at a fine scale less than a few micrometers. Therefore only PICC and RICC mechanisms are considered in the present study.

Roughness induced crack closure

The roughness profiles of the fracture surfaces have been recorded along the specimen thickness direction at different ΔK levels. Figure 7.a shows the profiles at $40 \text{ MPa}\sqrt{\text{m}}$ of aged and unaged elbow EK and of aged elbow n°1. Two levels of roughness can be distinguished : large differences in height (around 2 mm) which seem to correspond to changes of ferritic grains and smaller differences. Roughness has been quantified by the ratio of total profile length to specimen thickness (Figure 7.b). This ratio is increasing with ageing and with ΔK level which does not correspond to the tendency observed in crack closure levels. Therefore it seems that crack closure effect is not only induced by roughness.

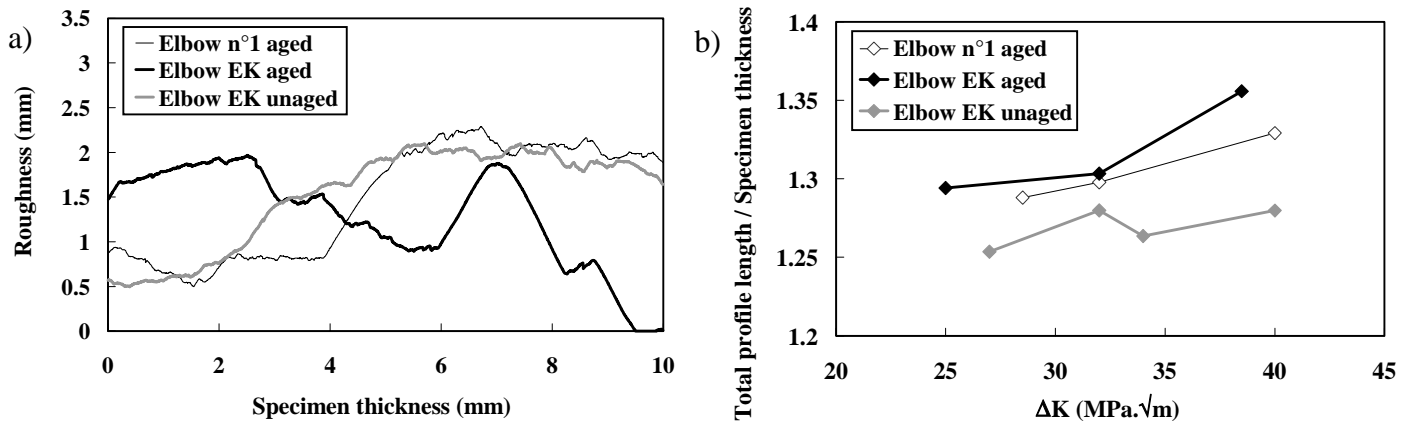


Figure 7 : Roughness of aged and unaged elbows n°1 and EK in equiaxed structure : a) fracture surface profiles at $\Delta K=40 \text{ MPa}\sqrt{\text{m}}$; b) ratio of total profile length to specimen thickness as a function of ΔK .

Plasticity induced crack closure

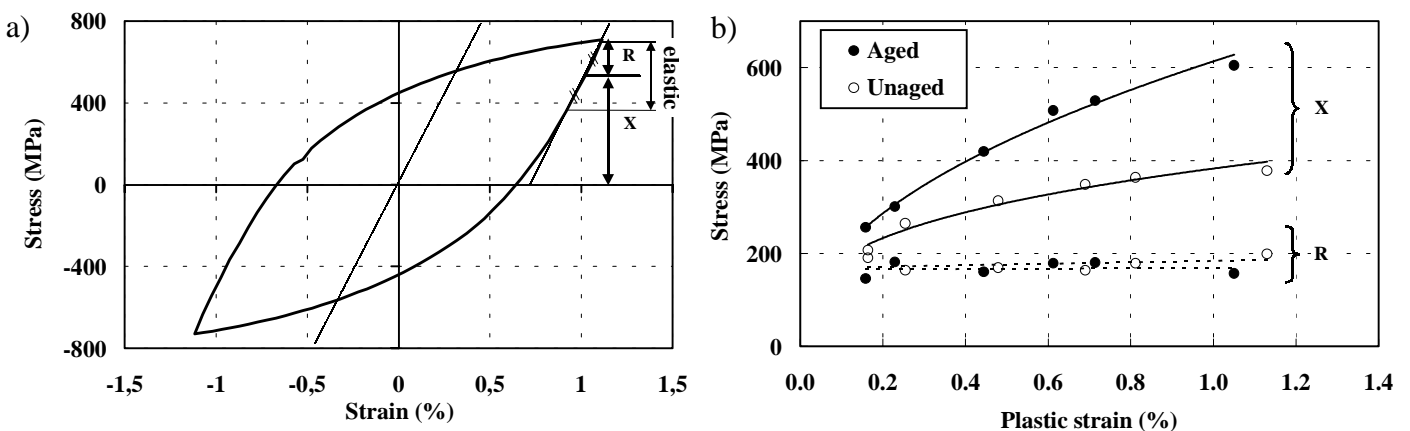


Figure 8 : Kinematic (X) and isotropic (R) hardening of elbow n°1 : a) definition of hardening on an hysteresis stress-strain loop; b) hardening as a function of cyclic plastic strain for aged and unaged materials.

Yield stress of aged and unaged materials are not sufficiently different to explain a difference in the plastic crack tip zone size. An attempt was made to explain the differences in crack closure levels by investigating the cyclic behaviour of aged and unaged materials. LCF tests showed that the materials exhibit cyclically

hardening. Kinematic (X) and isotropic (R) hardening can be measured from a stress-strain loop as explained in Figure 8.a. It appears that the isotropic hardening is the same for aged and unaged materials but that kinematic hardening is increasing with plastic strain and ageing (Figure 8.b). In these materials, it appears therefore that kinematic hardening is favourable to the development of crack closure effect. The effect of the constitutive equations on crack closure effect has been investigated recently using numerical modeling of crack propagation [10].

CRACK PROPAGATION MICRO-MECHANISMS

Fracture micro-mechanisms

The fracture micro-mechanisms of ferrite in duplex stainless steels depend on ageing. When aged, the ferrite fractures mainly by cleavage and between cleavage facets, by shearing (Figure 9.a). When unaged, the ferrite rupture is ductile.

The fracture micro-mechanism of austenite depends on ΔK and on the relative austenite crystallographic orientation to loading direction. At low ΔK , austenite fractures by "faceted" shearing along crystallographic planes if well oriented (Figure 9.b) and by shearing if not well oriented (Figure 9.a). At high ΔK , crack propagation occurs in austenite by ductile fatigue striation micro-mechanism.

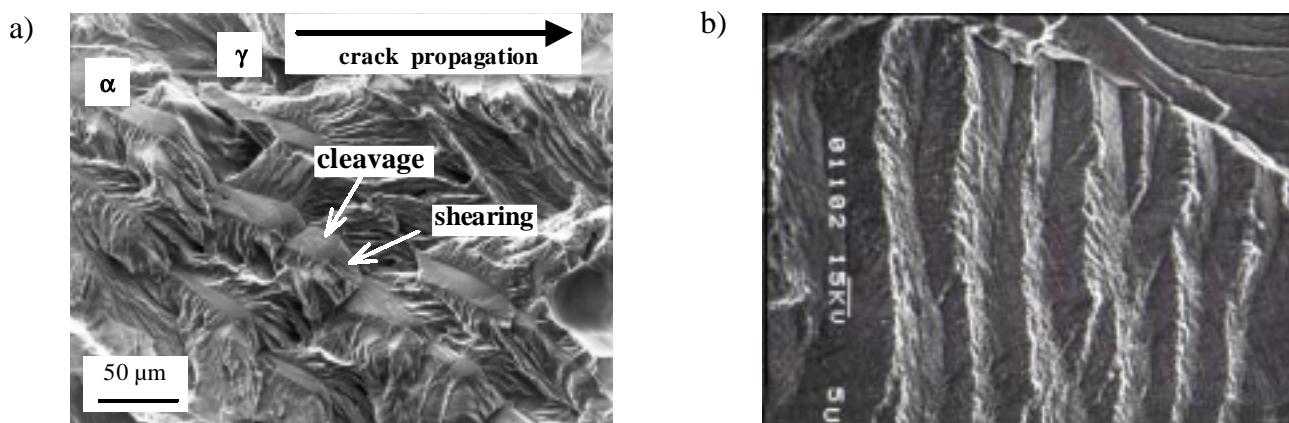


Figure 9 : Fracture morphologies in aged material: a) ferrite cleavage and shearing; b) steps in austenite.

Crack path

Surface ferrite fraction has been measured along the crack path on polished sections perpendicular to the crack plane of aged and unaged elbows n°1 and EK. This ferrite fraction was compared to the ferrite fraction measured on a line chosen randomly on a polished specimen. It appears that the two ferrite fractions are equivalent. As a consequence, it seems that no preferential path in ferrite or in austenite exists. Moreover, cleavage damage in ferrite ahead of the crack tip has been observed only rarely. Therefore, in this kind of materials and for the investigated ΔK range, the model according to which microcracks are formed ahead of the crack tip by cleavage within the ferrite phase forming an austenitic bridging zone is invalid [3].

The crack path has been studied by EBSD and it has been shown that, in aged materials, the macroscopic direction of the crack corresponds to a $\{100\}$ cleavage ferrite plane. In equiaxed material, ferrite grains are oriented randomly. The crack path changes of global direction when it changes of ferrite grain and many secondary cracks are created (Figure 10.a). The elongated direction of basalts corresponds to a $\{100\}$ α direction. So when the crack propagates in a plane perpendicular to basalts, it has no difficulty to find a $\{100\}$ plane in each basalt. This explains why the crack path is more regular with little secondary cracks (Figure 10.b). It might also explain the high crack propagation rates observed under these conditions. But, when the crack propagates in a plane parallel to basalts, it is very branched. In one area, three cracks can even be found (Figure 10.c). More investigations are required but it can be supposed that ferritic grain boundaries parallel to the crack plane can disturb crack propagation.

Looking more in detail, cracks in ferrite have been identified as cleavage $\{100\}$ planes (Figure 11). Crystallographic directions in austenite have been studied on secondary cracks. Figures 12.a and 9.a show that in this phase, the crack path is often changing of direction. Planes of type $\{111\}$, $\{110\}$ or $\{100\}$ have

been identified but it was difficult to establish a unique tendency. The classical model of crack propagation in Faced Cubic Centred metals [10] seems not respected in these dual phase materials (Figure 12.b).

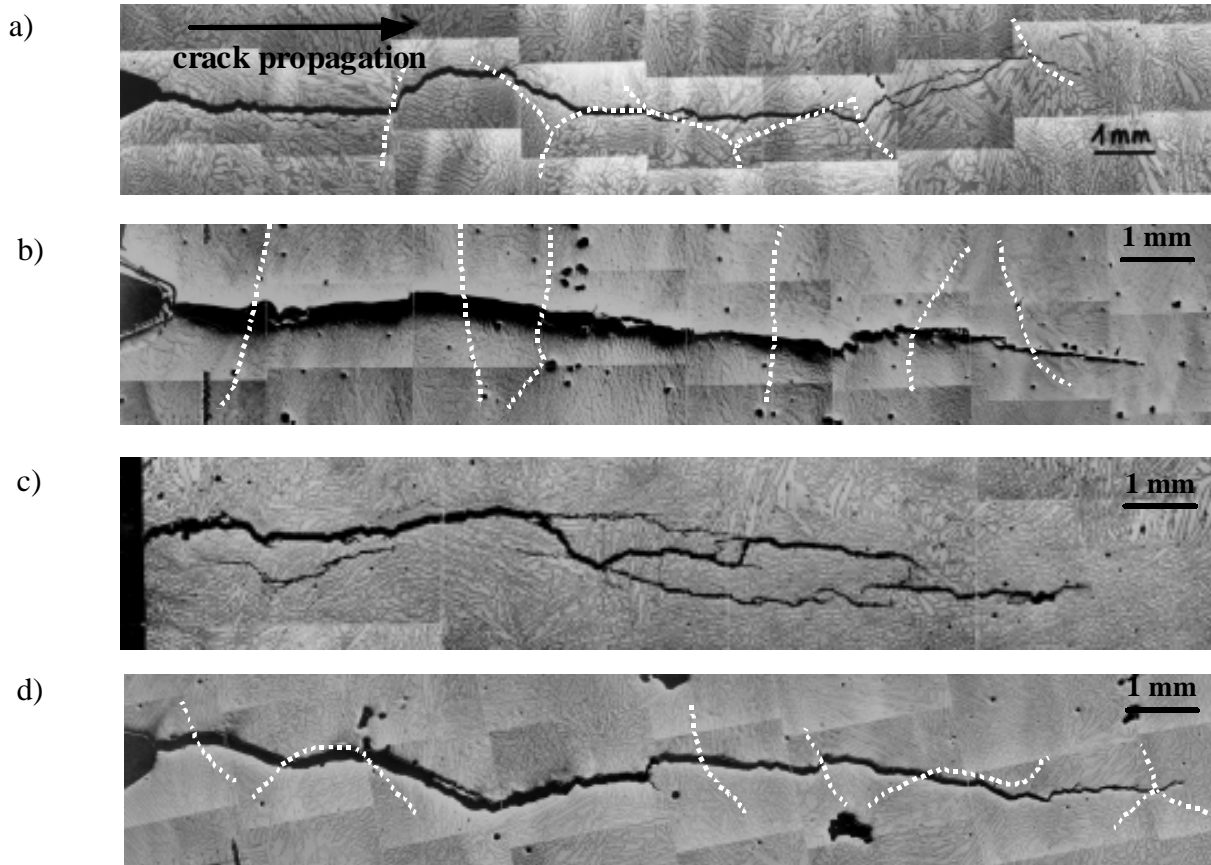


Figure 10 : Crack propagation in elbow n°1 : for aged material across equiaxed grains (a), in a plane perpendicular to basalts (b) and in a plane parallel to basalts (c); for unaged materials (d). Dotted lines represent the ferritic grain limits.

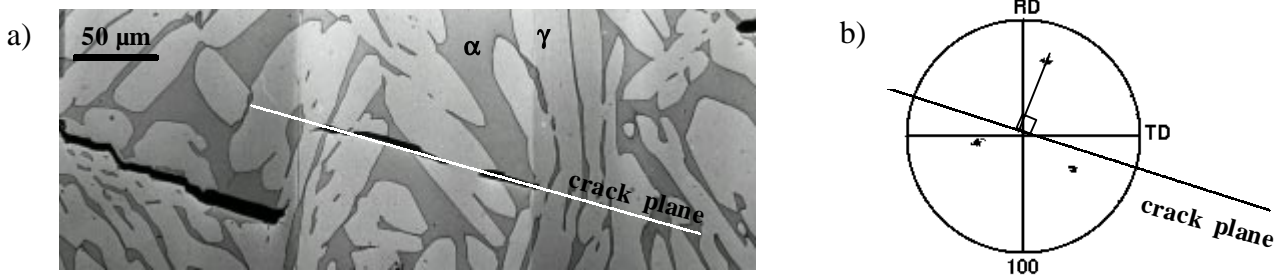


Figure 11 : Identification of the crack plane in ferrite of aged elbow n°1 : a) micrography; b) ferrite pole figure.

Unaged materials with equiaxed grains have also been studied. Crack also often changes of direction but secondary cracks are more rare (Figure 10.d). On the contrary to aged materials, the correlation between change of macroscopic direction and change of ferritic grain is not so easily observed. Macroscopic crack direction is close to $\{123\}$ planes. These planes are numerous so crack changes of macroscopic direction only when it is difficult to find this direction in the following grain.

CONCLUSION

→ Influence of ageing

FCGR increases with ageing when the aged material becomes brittle enough. But, when crack closure is taken into account, FCGR of aged and unaged materials are the same. This means that the influence of ageing on the FCGB mainly corresponds to a crack closure effect. Crack closure is induced by roughness but

also by cyclic plasticity at the crack tip. It is suggested that the differences in crack closure levels are produced by the differences in cyclic hardening behaviours.

→ **Influence of solidification induced structure**

In equiaxed grains or in a plane parallel to basalts, crack propagates at the same speed expressed as a function of ΔK . In a plane perpendicular to basalts, it propagates more quickly. The observation of crack path can give a qualitative explanation to this situation. Crack propagation in a plan perpendicular to basalts is very linear whereas the propagation path in equiaxed grains or in a plane parallel to basalts is very tortuous.

→ **Propagation mechanisms**

Ageing has an influence on ferrite fracture micro-mechanisms. Fracture is ductile when unaged and brittle when aged. It has been shown that there is no preferential crack path between the two phases and no shielding effect associated with fracture of ferrite ahead of the crack tip. In aged materials, the macroscopic crack propagation plane corresponds to the $\{100\}$ cleavage ferrite type whereas in unaged material, the fatigue crack preferentially propagates along $\{123\}$ ferrite type.

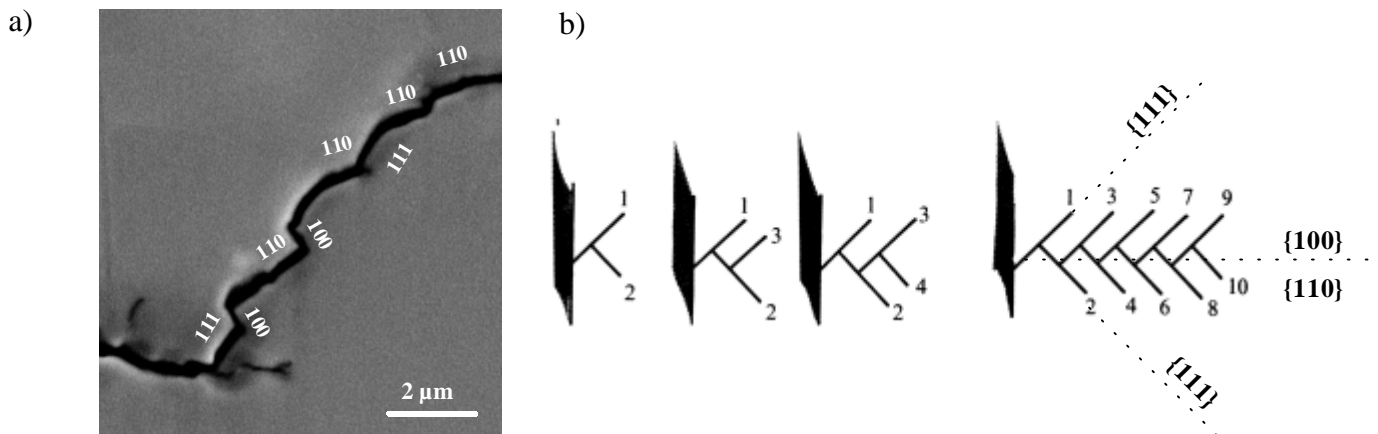


Figure 12 : a) Identification of the crack plane on a secondary crack in austenite;
b) classical model of fatigue crack propagation in FCC metals [8].

ACKNOWLEDGEMENTS

Financial support from Direction Supérieure des Installations Nucléaire is greatly acknowledged. The materials were provided by EDF and Framatome which are also acknowledged.

REFERENCES

1. Charles, J., Verneau, M. and Bonnefois, B. (1996). *Proc. 2nd European Cong. Stainless Steel'96*, Düsseldorf, pp. 97-103.
2. Danoix, F., Chambrelan, S., Massoud, J.P., Auger, P. (1992). *Collection de notes internes à la Direction des Etudes et Recherches*, EDF.
3. Marrow, T.J. and King, J.E. (1994). *Materials Science and Engineering*, A183, pp. 91-101.
4. Mateo, A., Ramirez, N., Llanes, L., Houbaert, Y. and Anglada, M. (1998). *Proc. ECF 12, Fracture from defects*, pp. 109-114
5. Iturgoyen, L. and Anglada, M. (1997). *Fatigue Fract. Engng. Mater. Struct.*, Vol 20, No 6, pp. 917-928.
6. Nyström, M. and Karlsson, B. (1996). *Materials Science and Engineering*, A215, pp. 26-38.
7. Kurdjumov, G.V. and Sachs, G. (1930). *Z. Phys.*64, 325.
8. Suresh, S. (1991). *"Fatigue of materials"*, Cambridge Solid State Science Series.
9. Pineau, A. and Pelloux, R., (1974). *Met. Trans.*, Vol. 5, pp. 1103.
10. Sansoz, F. (2000). Ph. D. Thesis, Ecole des Mines de Paris.